Nanoparticle Luminescence Thermometry

Shaopeng Wang, Sarah Westcott, and Wei Chen*

Nomadics, Inc., 1024 South Innovation Way, Stillwater, Oklahoma 74074

Received: July 3, 2002; In Final Form: August 23, 2002

A new concept of using luminescent nanoparticles for thermometry is described in this paper. To demonstrate this idea, the temperature-dependent emission characteristics of several luminescent nanoparticles have been investigated. The results show that some of them have a linear response above room temperature, which could be applied to temperature sensing. Semiconductor nanoparticles of CdTe and doped nanoparticles of ZnS:Mn^{2+} show a reversible linear temperature response over the physiological temperature range and have potential for biomedical thermometry. Double-doped nanoparticles of ZnS:Mn^{2+},Eu^{3+} show a different temperature response for each dopant; the ratio of their intensities provides a robust temperature measurement approach. Thermal instability of the nanoparticle stabilizer and nanoparticle surface defects is a possible reason for the irreversible thermal response of some nanoparticles.

I. Introduction

Temperature is a fundamental property of matter, and its measurement is often required for both scientific research and industrial applications. For industrial manufacturing, real-time temperature monitoring can be used to optimize processing, minimizing waste production and energy consumption. Spatially resolved temperature monitoring can establish regions of an integrated circuit in which heat builds up, and suggest improvements in design of the circuit or its cooling system. Monitoring the temperature of high-speed moving parts, such as turbine blades, can identify changes that signify a weakness in the part. In bioengineering and biochemistry, temperature changes of even a few degrees can mean the difference between life and death for a cell. Real time, precise in vivo monitoring of temperature is of paramount importance in many biomedical diagnostic and treatment processes.

Traditional methods of temperature measurement can be divided into two categories: contact methods, including thermocouples, thermistors, and resistance temperature detectors (RTDs); and noncontact methods such as measurement of emitted infrared light.[1] Thermistors, thermocouples, and RTDs all require electrical wiring, which is not suitable for applications in which electromagnetic noise is strong, sparks could be hazardous, the environment is corrosive, or parts are rapidly moving. Noncontact temperature measurement can be done by measurement of the infrared light that is emitted from a hot sample. One can either assume that the sample emits at the same rate as a blackbody or, for an accurate determination of temperature, the emissivity of the material must be known. For thermal imaging, the emissivity must be constant for all objects in the image. In addition, the infrared wavelengths typically used in determining temperature are absorbed by water vapor and by ordinary glass materials, preventing measurements through windows. Novel noncontact thermometry methods are being explored due to these limitations. Different physical properties are under investigation for thermometry applications, such as Rayleigh light scattering,[2] thermal reflection,[3] and magnetic resonance imaging (MRI) thermometry.[4,5] These methods are still in the proof of concept stage and their application is restricted because of the nature of the corresponding physical phenomena.

Fluorescence thermometry, using the fluorescence from luminescent materials to determine temperature, is a noncontact thermometry that can overcome many of the problems and limitations of the methods described above.[6] As the temperature of the phosphor changes, the intensity of the fluorescence, the decay lifetime of the fluorescence, the excitation spectra of the fluorescence, and the wavelength (or energy) of the fluorescence may all change. Because the fluorescence can be both excited and measured optically, fluorescence-based temperature sensors are advantageous compared to contact temperature sensors (such as thermocouples, thermistors, and RTDs) in applications where electromagnetic noise is strong or it is physically difficult to connect a wire (such as for spinning centrifuges or turbines or in wind tunnels). Emissivity does not affect the fluorescence signal, and wavelengths for fluorescence can be found for which glass and water are relatively transparent.

II. Concept of Nanothermometry

The fluorescence of phosphors is temperature-sensitive due to Boltzmann distribution statistics and depends on the band structure of each material.[7] For example, consider a material in which only radiative transitions from the bottom of the excited state to the ground state are possible at low temperature. However, at higher temperatures when thermal energy excites the electrons within the excited state, nonradiative transitions to the ground state become possible because the states overlap at a higher energy. The rate of nonradiative transitions is proportional to $\exp(-\Delta E/kT)$, where ΔE is the energy difference between the bottom of the excited state and the overlap point, k is Boltzmann's constant, and T is temperature. At higher temperatures, the nonradiative transition rate increases, decreasing the overall lifetime of the excited state and decreasing the intensity of emission from the excited state. Most materials have a more complex band structure with multiple excited bands that possess varying overlap energies, which may lead to a more complex temperature dependence.

* Corresponding author. Tel: 405-372-9535. Fax: 405-372-9537. E-mail: wchen@nomadics.com.

10.1021/jp026445m CCC: $22.00
Published on Web 10/05/2002

Conventional phosphors are made from crystalline semiconductor materials and typically have grain sizes of microns.[6] For noncontact thermometry, these grains are generally mixed with a binder material and coated on the surface of a part whose temperature is to be measured. The grain size limits resolution by scattering both the excitation light and emitted light. It also imposes a minimum thickness of phosphor coating of several microns on the sample. Thick coatings are disadvantageous because the phosphor coating may act as an insulating layer on the part's surface, giving results for temperature that cannot be applied to similar uncoated parts. However, these problems can be solved by using nanoparticles.

Nanoparticles are much smaller than conventional phosphors.[8,9] Using luminescent nanoparticles for temperature sensors should decrease light scattering and improve spatial resolution. Most light detection systems, including fluorescence thermometry, suffer from low resolution as a result of the scattering of both excitation and emission light. The light scattering is due to the phosphor grain size, the shape and the grain boundary, as well as surface roughness.[10] According to Raleigh's approximation, the intensity of scattered light from isotropic particles is approximately equal to the particle diameter to the sixth power.[11] This means that a 100-nm particle will scatter one million times more light than a 10-nm particle. Therefore, compared to the scattering in traditional micrometer-sized phosphors, the scattering of light in nanoparticles is close to zero. This suggests that much higher spatial resolution is possible by using nanoparticles for fluorescence thermometry or thermal imaging. Thin films of nanoparticles could be coated or sprayed on samples. Small size and ultrathin films should enable a faster equilibration time with an underlying sample and high sensitivity, accuracy, and spatial resolution. Nanoparticles are also suited for incorporation into coatings that would be applied to a part anyway, such as corrosion protection, making a "smart" material.

In addition, luminescent nanoparticles theoretically have higher quantum efficiency than conventional phosphors, making it possible to design and fabricate more sensitive temperature sensors. It is known that oscillator strength is a very important optical parameter that determines the absorption cross-section, recombination rate, luminescence efficiency, and the radiative lifetime in materials.[12] The oscillator strength of the free exciton is given by[13]

$$f_{ex} = \frac{2m}{\hbar}\Delta E|\mu|^2|U(0)|^2$$

where m is the electron mass, ΔE is the transition energy, μ is the transition dipole moment, and $|U(0)|^2$ represents the probability of finding the electron and hole at the same site (the overlap factor). In nanostructured materials, the electron−hole overlap factor increases largely due to quantum size confinement, thus yielding an increase in the oscillator strength. The oscillator strength is also related to the electron−hole exchange interaction that plays a key role in determining the exciton recombination rate. In bulk semiconductors, due to the extreme dislocation of the electron or hole, the electron−hole exchange interaction term is very small; while in molecular-size nanoparticles, due to the confinement, the exchange term should be very large. Therefore, we may expect a large enhancement of the oscillator strength from bulk to nanostructured materials.

Semiconductor nanoparticles can also be doped with impurities and have a strong luminescence as a result of the dopant. In doped semiconductors, excitons are bound to impurity centers.[14] Quantum size confinement will also enhance the bound exciton oscillator strength in doped nanoparticles.[15] The luminescence efficiency is also proportional to the exciton oscillator strength; therefore, it can be enhanced via quantum size confinement. Strong evidence for the above theory comes from our observations of ZnS:Mn^{2+} [16] and EuS[17] nanoparticles. The luminescence intensity of the 1 nm-sized ZnS:Mn^{2+} nanoparticles in zeolite-Y was much stronger than that of other larger nanoparticles.[16] Interestingly, bulk EuS at room temperature is not luminescent, but strong luminescence was observed when EuS nanoparticles were formed in zeolite.[17]

The radiative decay lifetime (τ) is closely related to the oscillator strength of a transition:[15]

$$\tau = 4.5(\lambda_A{}^2/nf)$$

where n is the refractive index and λ_A is the wavelength. Thus, the lifetime is shortened with decreasing size due to the increase of the oscillator strength, f. High efficiency with short decay times makes nanoparticles very good candidates for luminescence-based temperature sensors for high-speed monitoring.

A nanotechnology-based temperature sensing method, the Coulomb blockade thermometer (CBT), has been reported recently.[18] The CBT is based on the temperature dependence of the electrical conductance characteristics of nanofabricated tunnel junction arrays. This kind of thermometer is intended for cryogenic temperature monitoring, and it has been found insensitive to high magnetic fields. However, this method is only valid at temperatures below 30 K. Obviously, using luminescent nanoparticles has many advantages over the CBT of the nano-junction arrays, such as broad measurement range and pure optical detection.

An important application area of nanoparticle thermometry is in biological or biomedical applications for localized in vivo temperature probing, such as temperature monitoring during hyperthermia treatment. Polymer beads (80−90 nm in diameter) containing fluorescent molecules have been used to measure the temperature of a single living cell for disease and cancer diagnosis.[18] However, these fluorescent molecules are susceptible to photobleaching and not suitable for long-term monitoring. Nanoparticles are less susceptible to photobleaching,[20] are even smaller for injection into the cell, and can be readily conjugated to biomolecules, such as antibodies, to control where they will be placed for detection. MRI[4,5] has been recently explored for noninvasive in vivo temperature monitoring. Spatial resolution of a few mm^3 and temperature resolution of about 1 °C has been reported,[4] which is still far from that predicted for nanoparticle thermometry.

Temperature dependence of luminescent nanoparticles has been reported for the low-temperature range (below 300 K).[21−24] Due to quantum confinement, the thermal behavior of nanoparticle luminescence is more complicated than that of conventional phosphors. There is a need to consider the processes of nonradiative relaxation via phonon coupling, exciton thermal dissociation (binding energy), energy transfer, carrier trapping, and temperature dependence of the absorption spectra.[23] Luminescence thermal behavior of nanoparticles has been found to be size dependent.[24] To the best of our knowledge, the temperature dependence of nanoparticle luminescence above room temperature, which is important to many thermometry applications, has not been previously reported.

To demonstrate our concepts of luminescent nanoparticle thermometry, we have measured the temperature response of several luminescent nanoparticle samples above room temperature. The tested nanoparticles may be characterized into three classes: semiconductor nanoparticles, such as CdTe; single-

doped semiconductor nanoparticles, such as ZnS:Mn^{2+}, Zeolite−Eu^{3+}, BaFBr:Eu^{2+}; and double-doped nanoparticles, such as ZnS:Mn^{2+},Eu^{3+}. The fluorescence emission spectra of these samples were measured over the temperature range from room temperature up to 150 °C.

III. Materials and Methods

All chemicals used were purchased from commercial sources. Our recipes for making II−VI semiconductor nanoparticles are similar to those reported in the literature.[16,25−29] However, some changes were made to improve nanoparticle quality.

The recipe for making CdTe nanoparticles has been reported elswhere.[30] The size of the nanoparticles used in these experiments is ∼4 nm as observed by a high-resolution transmission electron microscope (HRTEM). Most of these nanoparticles are spherical in shape. The [1,1,1] lattice spacings can be seen from the HRTEM images and the spacing found is about 0.36 nm, which is in agreement with the [1,1,1] spacing of cubic CdTe of 0.374 nm.[23]

The recipes for making Mn^{2+}-, Er^{3+}-, and Eu^{3+}-doped ZnS nanoparticles are similar.[16,28,29] The recipe for making uncapped ZnS:Mn^{2+} nanoparticles is as follows. A four-neck flask was charged with 400 mL deionized water and was stirred under N_2 for 2.5 h. An aqueous solution of 1.6 g Na_2S and an aqueous solution of 5.8 g $Zn(NO_3)_2.6(H_2O)$ and 0.26 g $Mn(NO_3)_2$ (Mn^{2+}/Zn^{2+} molar ratio 5:95) were prepared and added to the first solution simultaneously at the same rate via two different necks. After the addition, the resulting solution was stirred constantly under N_2 at 80 °C for 24 h and a transparent colloid of ZnS:Mn^{2+} was formed. The pH value of the final solution was 2.4. This relatively low pH value is required to prevent the precipitation of unwanted Mn species. The nanoparticles were separated from solution by centrifugation and dried in a vacuum at room temperature. The particle size is around 10 nm as determined by HRTEM.

To make BaFBr:Eu^{2+} nanoparticles in MCM-41, bulk BaFBr:Eu^{2+} powder was made by solid-state diffusion at 800 °C for 2 h. Then, BaFBr:Eu^{2+} powder and MCM-41 powder (ratio of BaFBr:Eu^{2+}:MCM-41 was 5:95) were mixed and heated at 600 °C under N_2 for 2 h. The particles formed within the channels of MCM-41 are around 4 nm in size.[31] Nanoclusters of Eu^{3+} doped in Zeolite-Y were synthesized according to the method described previously.[32]

To prepare samples for luminescence measurements, the nanoparticles were dispersed in acetone, dropped onto a glass cover slide, and air-dried to form a thin solid film. The glass cover slide was then placed on a shop-built sample holder with temperature control. The fluorescence spectra were measured with a fluorometer (FluoroMax-2 from Jobin Yvon-Spex). The time interval between the measurements of two different temperatures is about 5 min, allowing the temperature control system to stabilize the temperature at the desired level.

IV. Results and Discussion

In Figure 1 (top and middle), the fluorescence peak intensity of uncapped ZnS:Mn^{2+} nanoparticles of 10 nm diameter at wavelengths of 589 nm (corresponding to the $^4T_1 \rightarrow {}^6A_1$ transition of Mn^{2+})[16] shows a linear and reversible response to temperature between 30 and 150 °C in several heating−cooling cycles. The change of intensity is nearly 0.5% per °C. The peak position also shows a slight blue shift, about 0.05 nm/°C. Interestingly, nanoparticles of similar composition, ZnS:Mn^{2+},-Er^{3+}, but with poly(vinyl alcohol) as a stabilizer and a diameter of 5 nm show irreversible quenching of the Mn^{2+} fluorescence

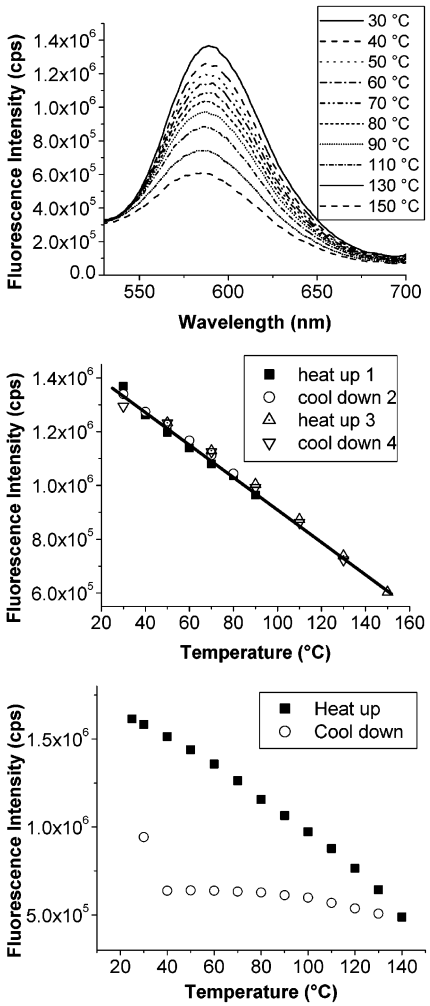

Figure 1. Top: Fluorescence spectra of 10 nm ZnS:Mn^{2+} nanoparticles without organic stabilizer, at different temperatures, from top to bottom: 30−150 °C; excitation wavelength: 360 nm. Middle: Fluorescence peak intensity at 589 nm ($^4T_1 \rightarrow {}^6A_1$) as a function of temperature for 10 nm ZnS:Mn^{2+} nanoparticles without stabilizer. Bottom: Fluorescence peak intensity at 593 nm as a function of temperature for 5 nm ZnS:Mn^{2+},Er^{3+} nanoparticles with poly(vinyl alcohol) as stabilizer.

upon heating and cooling (Figure 1, bottom). Possible explanations for this could be that the organic stabilizer partially oxidizes and decomposes or that the smaller nanoparticles are less stable due to their large surface energy. Further evidence to support this argument comes from the CdTe nanoparticle results, as discussed in the next paragraph.

The fluorescence peak intensity of CdTe nanoparticles is linearly and reversibly proportional to the temperature in the 30−60 °C range (Figure 2, top and center), with a large response slope of 1.1% per °C. However, higher temperatures (140 °C) induced an irreversible quenching effect (bottom). A 4 nm irreversible blue shift of CdTe emission peak was also observed after the high-temperature measurement, which was not observed after heating in the 30−60 °C range. Again, this may be due to the oxidization and decomposition of the organic stabilizer of the nanoparticles (thioglycolic acid), which has a boiling point of 96 °C.

Both CdTe and ZnS:Mn^{2+} nanoparticles could be suitable candidates for biomedical applications (in vivo and in vitro thermometry) due to their large and linear intensity shift over the physiological and hyperthermia temperature range.[33] The −COOH group of the thioglycolic acid stabilized CdTe nano-

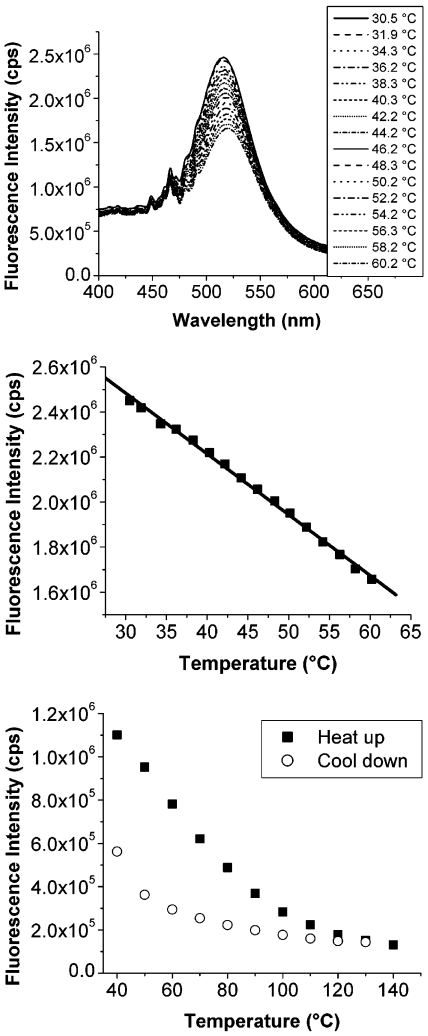

Figure 2. Top: Fluorescence spectra of CdTe nanoparticles at different temperatures, from top to bottom: 30−60 °C; excitation wavelength: 350 nm. Middle: Fluorescence peak intensity (518 nm) of CdTe nanoparticles as a function of temperature. Bottom: Fluorescence peak intensity of CdTe nanoparticles as a function of temperature with an irreversible effect after heating to 140 °C.

particle can be used to easily conjugate to the amine group of biological molecules (e.g., antibodies), such as by the widely used EDC/NHS reaction.[34,35]

In Figure 3, the peak intensity of the fluorescence of BaFBr:Eu^{2+} nanoparticles in MCM-41 responds linearly and reversibly to temperatures between 30° and 150 °C at a rate of 0.2% per °C. The emission band at 388 nm corresponds to the $4f^6 5d^1 \rightarrow 4f^7(^8S_{7/2})$ transition of Eu^{2+}.[17] These nanoparticles show exceptional reversibility.

We found that some nanoparticles have a permanent luminescence enhancement after heating. For the example shown in Figure 4, the intensities of the two major emission peaks at 588 and 611 nm (corresponding to the $^5D_0 \rightarrow {}^7F_1$ and $^5D_0 \rightarrow {}^7F_2$ transition, respectively[31,32]) of Eu^{3+} nanoparticles in zeolite are enhanced irreversibly after heating to 140 °C (top right). This may be due to the heat-induced curing effect, since it is stabilized after an extended heating time, as shown in Figure 4, bottom. We also found a similar heat-induced luminescence enhancement effect for several other doped nanoparticles, such as ZnS:Eu^{3+} and Y_2O_3:Eu^{3+}. We know that some doped nanoparticles can be UV-cured to enhance the quantum efficiency.[36] Our hypothesis is that the heating process cured the

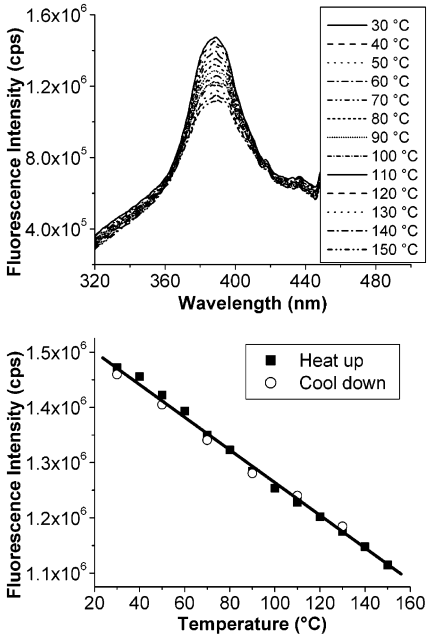

Figure 3. Top: Fluorescence spectra of BaFBr:Eu^{2+} nanoparticles in MCM-41 at different temperatures, from top to bottom: 30−150 °C; excitation wavelength: 280 nm. Bottom: Fluorescence peak intensity (388 nm, $4f^6 5d^1 \rightarrow 4f^7(^8S_{7/2})$) of BaFBr:$Eu^{2+}$ nanoparticles as a function of temperature, during a heat-up and cool cycle. Squares: heating; circles: cooling.

defects on the nanoparticle surface and increased the quantum efficiency of the luminescence.

In Figure 5, the fluorescence of double-doped nanoparticles of ZnS:Mn^{2+},Eu^{3+} is shown. The shape of the fluorescence spectrum of this double-doped nanoparticle depends on the excitation wavelength. When excited at 394 nm, the emission spectrum is mainly contributed by Eu^{3+}, with the dominant peak position at 612 nm ($^5D_0 \rightarrow {}^7F_2$). When excited at 360 nm, the emission spectrum is mainly due to Mn^{2+}, with a peak position at 595 nm ($^4T_1 \rightarrow {}^6A_1$). Emission intensity of Eu^{3+} is less temperature-dependent than that of Mn^{2+}. This is probably due to the difference in the transition properties of the two ions. The emission of Eu^{3+} is due to f−f transition while the emission of Mn^{2+} is due to d−d transition. As a result of the shielding of their f electrons, f−f transitions are extremely insensitive to their environment, and have high thermal stability.[37,38] In contrast, d−d transitions of Mn^{2+} are largely affected by the crystal field and sensitive to the environment.[36] The ratio of the two peaks has an approximately linear response to temperature changes over the range of 30−150 °C. The measurement of peak ratio could be much easier and more reliable than a single peak intensity measurement in practical applications. This is because variations of the optical path, such as the bend of an optical fiber or skin penetration, could change the detected fluorescence intensity easily, but the ratio of the two peak intensities is much less dependent on such factors.

The thermal behavior of fluorescent nanoparticles that we observed all show decreased intensity at higher temperatures, which follows the same trend as bulk fluorophores. However, the linear relationship between the nanoparticle luminescence intensity and temperature is different from bulk materials, for which the intensity decays exponentially with increasing temperature due to the increase of the nonradiative relaxation. The linear relationship is in agreement with the low-temperature thermal behavior of nanoparticle fluorescence reported in the literature.[23,24] Energy transfer from the excited states to trapped

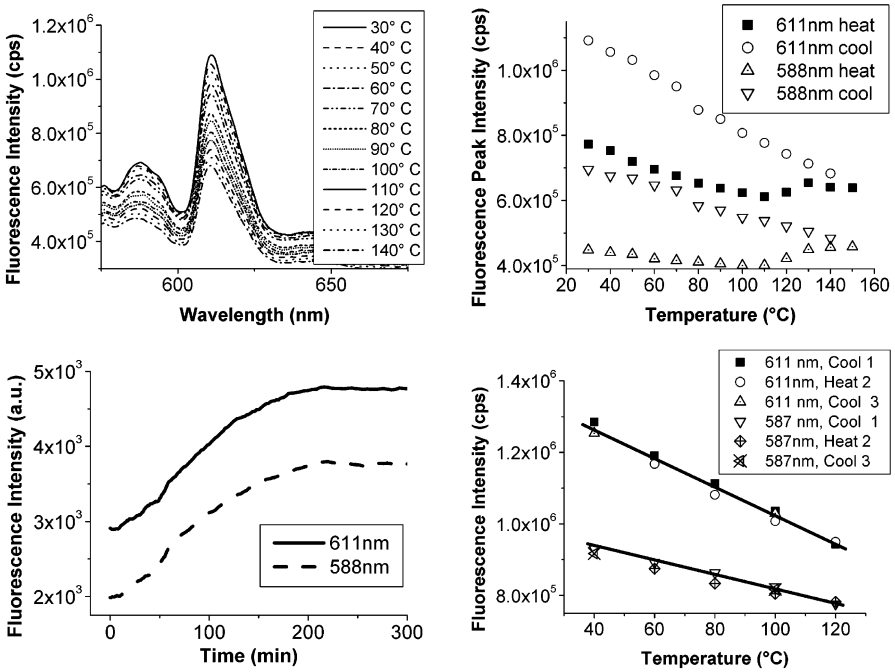

Figure 4. Top left: Fluorescence spectra of Eu^{3+} nanoclusters in zeolite at different temperatures, from top to bottom: 30−140 °C, excitation wavelength: 392 nm. Top right: Fluorescence peak intensity of Eu^{3+} nanoparticles at 611 and 588 nm (corresponding to $^5D_0 \rightarrow {}^7F_2$ and $^5D_0 \rightarrow {}^7F_1$ transition, respectively) as a function of temperature. Bottom left: Fluorescence peak intensity as a function of time during heat curing. Bottom right: Fluorescence peak intensity (611 and 588 nm) of Eu^{3+} nanoparticles as a function of temperature, after heat curing at 120 °C for 5 h.

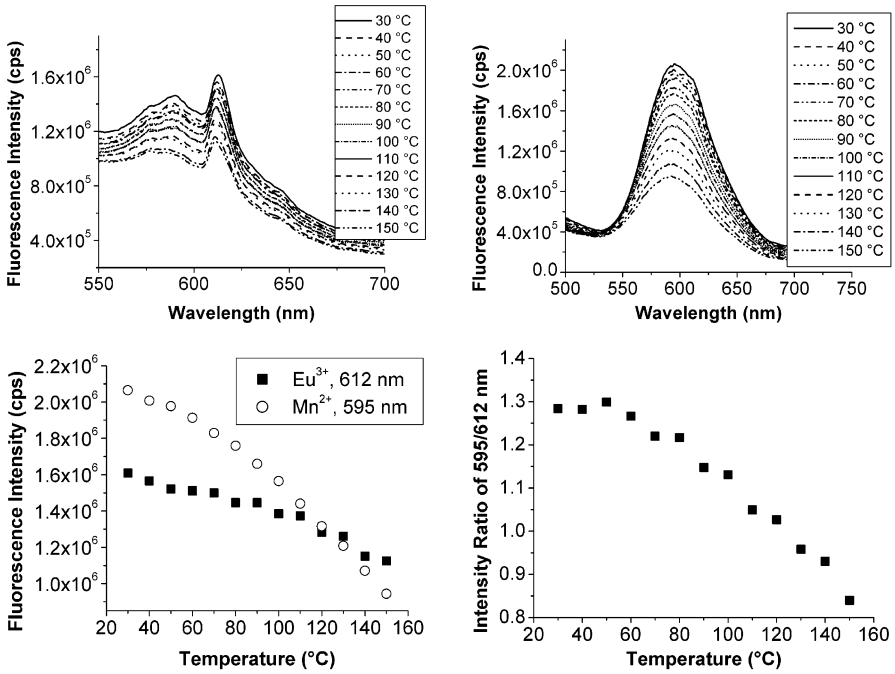

Figure 5. Top: Fluorescence spectra of ZnS:Mn^{2+},Eu^{3+} nanoparticles at different temperatures, from top to bottom: 30−150 °C. Top left: Excitation wavelength: 394 nm, peak 612 nm due to $5D_0 \rightarrow 7F_2$ transition of Eu^{3+}. Top right: Excitation wavelength: 360 nm, peak 595 nm due to $^4T_1 \rightarrow {}^6A_1$ transition of Mn^{2+}. Bottom left: Fluorescence peak intensity as a function of temperature. Square: 612 nm emission (394 nm excitation), round: 595 nm emission (360 nm excitation). Bottom right: intensity ratio of the two peaks (595 nm/612 nm) as a function of temperature.

surface states, which must be considered in nanoparticles, is less effective at higher temperatures leading to an increase in the fluorescence intensity.[23] In addition, thermoluminescence from nanoparticles also needs to be considered.[39] Electrons and/or holes may be trapped at the surface states or defects of nanoparticles during preparation.[39] During heating, the trapped carriers may escape from their traps and recombine to give luminescence which is called thermoluminescence. Over a certain temperature range, the thermoluminescence intensity increases with increasing temperature. Overall, thermoluminescence and decreased trapping at surface states may partially compensate for the exponential decay due to the increased nonradiative relaxation and lead to a different relationship. Due to the limited temperature range tested, we also may see a slow exponential decay as a linear relationship. Further investigations are needed to fully understand the mechanism of the decrease. The observed shift of the Mn^{2+} $^4T_1 \rightarrow {}^6A_1$ emission of ZnS:Mn^{2+} nanoparticles to shorter wavelengths at higher temperatures also follows the same trend as reported low-temperature measurements, and can be explained by the decrease in the

crystal field strength at higher temperature, which moves the emitting state ($^4T_1$) to higher energies.[23]

The signal-to-noise ratio of our fluorescence spectrometer is approximately 5000:1, which means that it can detect a 0.02% change of fluorescence intensity. The CdTe nanoparticles have a temperature dependence of 1.101 ± 0.015% per °C, calculated from the linear regression of the 30−60 °C results. Therefore, the resolution could be as good as 0.02 °C in principle. For the relatively small changes of BaFBr:Eu^{2+} nanoparticles of 0.207 ± 0.006% per °C, resolution of 0.1 °C is still theoretically possible.

Although the results above only demonstrated the thermal response of fluorescence intensity and band changes, it should be pointed out that other fluorescence characteristics such as fluorescence lifetime should respond to temperature change too, as for conventional fluorophores.

It may also be possible to synthesize structures in which fluorescence resonance energy transfer (FRET) occurs between two different dopants in a nanoparticle or between two nanoparticles of different sizes or compositions.[40] FRET can occur when the emission spectrum of the higher energy emitter overlaps with the absorption spectrum of the lower energy emitter. The FRET rate is dependent inversely on the distance between the donor and emitter to the sixth power.[41] Therefore, if the distance is changed slightly due to thermal expansion of the material between the dopants or nanoparticles, the energy transfer rate will be changed greatly. This provides a good method for temperature or pressure sensors.[40]

Another potential approach to nanoparticle fluorescence thermometry is the use of upconversion luminescence in which the excitation wavelength is longer than the emission wavelength. Strong upconversion luminescence has been observed in certain nanoparticles. For example, two-photon-induced upconversion luminescence was first observed in ZnS:Mn^{2+} and ZnS:Mn^{2+},Eu^{3+} nanoparticles by Chen et al.[23,42] These observations revealed that the upconversion luminescence intensity of ZnS:Mn^{2+} nanoparticles is highly temperature-dependent. A close-to-linear temperature dependence of the upconversion intensity was observed in ZnS:Mn^{2+} nanoparticles formed in zeolite-Y.[23] This indicates that the upconversion luminescence of nanoparticles can be used for temperature sensors. One advantage of upconversion for temperature sensing or imaging, compared with fluorescence, is that the emission background from the surroundings that occurs with fluorescence can be avoided in upconversion.[43] This is particularly interesting in biological or biomedical applications, because many biological components such as cells and tissues have strong autofluorescence upon excitation with UV light.

V. Conclusions

The temperature dependence of the fluorescence emission spectra of different luminescent nanoparticles has been investigated. The results show that some of them have a linear response above room temperature. CdTe and ZnS:Mn^{2+} nanoparticles show a reversible linear temperature response over the physiological temperature range with a theoretical temperature sensing resolution up to 0.02 °C; therefore these nanoparticles have the potential to be used for biomedical thermometry applications, such as temperature monitoring during hyperthermia treatment. Double-doped nanoparticles of ZnS:Mn^{2+},Eu^{3+} show a different temperature response for each dopant, as a result of their difference in transition properties. The ratio of the intensities of the two emissions should be insensitive to variations in intensity as a result of factors other than temperature shift. While some nanoparticles have a reversible thermal response, several nanoparticles show an irreversible thermal response. The irreversible quenching could be due to the thermal oxidization and decomposition of the nanoparticle stabilizers, and the irreversible luminescence enhancement could be due to the thermal curing of nanoparticle surface defects. Because of their small size and low light scattering, nanoparticles may provider higher resolution and sensitivity over traditional phosphors for standoff thermometry.

References and Notes

(1) Bentley, R. E. *Temperature and Humidity Measurement*; Springer: Singapore, 1998. Also, http://www.temperatures.com, and references therein.

(2) Horton, J. F.; Peterson, J. E. *J. Heat Transfer* **2000**, *122*, 165−170.

(3) Fan, C. H.; Longtin, J. P. *J. Heat Transfer* **2000**, *122*, 757−762.

(4) Olsrud, J.; Wirestam, R.; Brockstedt, S.; Nilsson, A. M. K.; Tranberg, K.-G.; Stahlberg, F.; Persson, B. R. R. *Phys. Med. Biol.* **1998**, *43*, 2597−2613.

(5) Hentschel, M.; Dreher, W.; Wust, P.; Roll, S.; Leibfritz, D.; Felix, R. *Phys. Med. Biol.* **1999**, *44*, 2397−2408.

(6) Allison, S. W.; Gillies, G. T. *Rev. Sci. Instrum.* **1997**, *68*, 2615−2650.

(7) Grattan K. T. V.; Zhang, Z. Y. *Fiber Optic Fluorescence Thermometry*; Chapman and Hall: London, 1995.

(8) Alivisatos, A. P. *Science* **1996**, *271*, 933−937.

(9) Alivisatos, A. P. *J. Phys. Chem.* **1996**, *100*, 13226−13239.

(10) Thoms, M. *Appl. Opt.* **1996**, *35*, 3702−3714.

(11) Kaszuba, M. *J. Nanoparticle Res.* **1999**, *1*, 405−409.

(12) Wang, Y. *Adv. Photochem.* **1995**, *19*, 179.

(13) Knox, R. S. *Theory of Excitons*, Solid State Physics Supplement 5; Academic Press: New York, 1963; p 120.

(14) Swiatek, K.; Godlewski, M.; Hommel, D. *Phys. Rev. B* **1990**, *42*, 3628−3633.

(15) Rashba, E. I.; Gurgenishvili, G. E. *Sov. Phys. Solid State* **1962**, *4*, 759.

(16) Chen, W.; Sammynaiken, R.; Huang, Y. *J. Appl. Phys.* **2000**, *88*, 5188−5193.

(17) Chen, W.; Zhang, X. H.; Huang, Y. *Appl. Phys. Lett.* **2000**, 76, 2328−2330.

(18) Kauppinen, J. P.; Loberg, K. T.; Manninen, A. J.; Pekola, J. P. *Rev. Sci. Instrum.* **1998**, *69*, 4166−4175.

(19) Simon, S. M. *Fluorescent Bead for Determining the Temperature of a Cell and Methods of Use Thereof*; U.S. Patent 6,132,958, issued Oct. 17, 2000.

(20) Chan, W. C. W.; Nie, S. *Science* **1998**, *281*, 2016−2018.

(21) Yu, J. Q.; Liu, H. M.; Wang, Y. Y.; Fernandez, F. E.; Jia, W. Y. *J. Lumin.* **1998**, *76&77*, 252.

(22) Tanaka, M.; Masumoto, Y. *Chem. Phys. Lett.* **2000**, *324*, 249−254.

(23) Joly, G.; Chen, W.; Roark, J.; Zhang, J. Z. *J. Nanosci. Nanotech.* **2001**, *1*, 295−301.

(24) Sui, F. H.; Ma, B. S.; Fan, Z. L.; Ding, K.; Li, G. H.; Chen, W. *J. Phys.: Condens. Matter*, in press.

(25) Rajh, T.; Micic, O. I.; Nozik, A. J. *J. Phys. Chem.* **1993**, *97*, 11999−12003.

(26) Rogach, L.; Katsikas, L.; Kornowski, A.; Su, D.; Eychmuller, A.; Weller, H. *Ber. Bunsen-Ges. Phys. Chem.* **1996**, *100*, 1772−1778.

(27) Stirner, T.; Kirkman, N. T.; May, L.; Ellis, C.; Nicholls, J. E.; Kelly, S. M.; O'Neill, M.; Hogg, J. H. C. *J. Nanosci. Nanotechnol.* **2001**, *1*, 451−455.

(28) Chen, W.; Sammynaiken, R.; Huang, Y.; Malm, J.-O.; Wallenberg, R.; Bovin, J.-O.; Zwiller, V.; Kotov, N. A. *J. Appl. Phys.* **2001**, *89*, 1120−1129.

(29) Chen, W.; Malm, J.-O.; Zwiller, V.; Huang, Y.; Liu, S. M.; Wallenberg, R.; Bovin, J.-O.; Samuelson, L. *Phys. Rev. B* **2000**, *61*, 11021−11024.

(30) Chen, W.; Grouquist, D.; Roark, J. *J. Nanosci. Nanotechnol.* **2002**, *2*, 47−53.

(31) Chen, W.; Joly, A. G.; Kowalchuk, C. M.; Malm, J.-O.; Huang, Y.; Bovin, J.-O. *J. Phys. Chem. B* **2002**, *106*, 7034−7041.

(32) Chen, W.; Sammynaiken, R.; Huang, Y. *J. Appl. Phys.* **2000**, *88*, 1424−1431.

(33) Hergt, R.; Andra, W.; d'Ambly, C. G.; Hilger, I.; Kaiser, W. A.; Richter, U.; Schmidt, H.-G. *IEEE Trans. Magn.* **1998**, *34*, 3745−3754.

(34) Hermanson, G. T. *Bioconjugate Techniques*; Academic Press: San Diego, 1996.

(35) Wang, S.; Mamedova, N.; Kotov, N. A.; Chen, W.; Studer, J. *Nano Letters* **2002**, *2*, 817−822.
(36) Bhargava, R. N.; Gallagher, D.; Hong X.; Nurmikko, A. *Phys. Rev. Lett.* **1994**, *72*, 416−419.
(37) Lenth, W.; Macfarlane, R. M. *Opt. Photon. News* **1992**, *3*, 8.
(38) Scheps, R. *Prog. Quantum Electron.* **1996**, *20*, 271−358.
(39) Chen, W.; Wang, Z.; Lin, Z.; Lin, L. *Appl. Phys. Lett.* **1997**, *70*, 1465−1467.
(40) Chen, W.; Wang, S.; Westcott, S. *Nanoparticle Thermometry and Pressure Sensing*; U.S. provisional patent, filed on June 12, 2002.
(41) Dexter, D. L. *J. Chem. Phys.* **1953**, *21*, 836.
(42) Chen, W.; Joly, A. G.; Zhang, J. Z. *Phys. Rev. B* **2001**, *64*, 0412021-4(R).
(43) dos Santos, P. V.; de Araujo, M. T.; Gouveia-Neto, A. S.; Madeiros Neto, J. A.; Sombra, A. S. B. *IEEE J. Quantum Elec.* **1999**, *35*, 395−399.